



Contents lists available at ScienceDirect

Vision Research

journal homepage: www.elsevier.com/locate/visres

Testing vision with angular and radial multifocal designs using Adaptive Optics

Maria Vinas*, Carlos Dorronsoro, Veronica Gonzalez, Daniel Cortes, Aiswaryah Radhakrishnan, Susana Marcos

Institute of Optics, Spanish National Research Council (CSIC), Serrano, 121, Madrid 28006, Spain

ARTICLE INFO

Article history:

Received 9 February 2016
Received in revised form 5 April 2016
Accepted 18 April 2016
Available online xxx

Keywords:

Presbyopia
Multifocal corrections
Adaptive Optics
Spatial Light Modulators

ABSTRACT

Multifocal vision corrections are increasingly used solutions for presbyopia. In the current study we have evaluated, optically and psychophysically, the quality provided by multizone radial and angular segmented phase designs. Optical and relative visual quality were evaluated using 8 subjects, testing 6 phase designs. Optical quality was evaluated by means of Visual Strehl-based-metrics (VS). The relative visual quality across designs was obtained through a psychophysical paradigm in which images viewed through 210 pairs of phase patterns were perceptually judged. A custom-developed Adaptive Optics (AO) system, including a Hartmann-Shack sensor and an electromagnetic deformable mirror, to measure and correct the eye's aberrations, and a phase-only reflective Spatial Light Modulator, to simulate the phase designs, was developed for this study. The multizone segmented phase designs had 2–4 zones of progressive power (0 to +3D) in either radial or angular distributions. The response of an “ideal observer” purely responding on optical grounds to the same psychophysical test performed on subjects was calculated from the VS curves, and compared with the relative visual quality results. Optical and psychophysical pattern-comparison tests showed that while 2-zone segmented designs (angular & radial) provided better performance for far and near vision, 3- and 4-zone segmented angular designs performed better for intermediate vision. AO-correction of natural aberrations of the subjects modified the response for the different subjects but general trends remained. The differences in perceived quality across the different multifocal patterns are, in a large extent, explained by optical factors. AO is an excellent tool to simulate multifocal refractions before they are manufactured or delivered to the patient, and to assess the effects of the native optics to their performance.

© 2016 Elsevier Ltd. All rights reserved.

1. Introduction

Restoring eye functionality in presbyopia, the age-related loss of the accommodative amplitude of the human eye (Glasser & Campbell, 1998), requires providing some near-vision functionality to presbyopic patients that have lost the ability to accommodate. Multifocal vision corrections are increasingly used solutions for presbyopia, which work by the principle of simultaneous vision, projecting simultaneously focused and defocused images on the retina. These corrections generally provide multifocality at the expense of reducing optical quality at all distances. There are multiple multifocal designs, working on diffractive or refractive principles, including bifocal concentric designs, bifocal angular designs, diffractive bifocal and trifocal designs, extended depth of focus

designs with smooth profiles or hybrid designs, producing different foci (Charman, 2014).

Diffractive IOLs use diffractive optics whereby constructive and destructive interferences produce near and far foci (Davison & Simpson, 2006), and multifocality is achieved at any pupil diameter (Charman, 2014). However, they are subject to diffractive effects by multiple orders as well as to chromatic effects, as the inferences are wavelength-dependent. Different design strategies, such as reducing the height of the diffractive phase in the lens periphery (apodization), to increase efficiency at far (i.e. RESTOR diffractive bifocal IOL, Alcon Research Labs, USA) (Davison & Simpson, 2006), or adjusting the height of the diffractive phase steps across the entire lens to produce an additional focus at intermediate distances (Charman, 2014; Schmidinger et al., 2006). Examples of trifocal diffractive IOL designs include the FineVision lens (Physiol, Belgium), in which the diffractive surface profile is designed to concentrate light into near (+3.5 D), intermediate

* Corresponding author.

E-mail address: maria.vinas@io.cfmac.csic.es (M. Vinas).

(+1.75 D) and distant foci (Charman, 2014; Gatinel, Pagnouille, Houbrechts, & Gobin, 2011) and the AT LISA tri (Zeiss, Germany), where the diffractive profile generates two foci for near and intermediate (+3.33 D and +1.66 D) respectively (Mojzsis, Majerova, Hrkova, & Pinero, 2015).

Some multifocal refractive contact and intraocular lens aim at expanding depth of focus (DoF) using different strategies, most frequently using aspheric profiles. Aspheric multifocal designs are common in contact lenses (Yi, Iskander, & Collins, 2011) and are being introduced in some IOLs (for example the W-IOL by Mediem, Switzerland). In this approach, it has been noted that the specific amount aberration to be introduced is critical and may be subject-specific (Dorronsoro, Gonzalez-Anera, Gonzalez, Llorente, & Marcos, 2004). Recently, using an optical design multi-configuration approach, IOLs with surfaces optimized to enhance retinal image quality over a certain range of focus have been presented (Fernandez, Barbero, Dorronsoro, & Marcos, 2013). Several studies have used Adaptive Optics (AO) to simulate the effects of inducing different levels of spherical aberration in experimental settings (Piers, Fernandez, Manzanera, Norrby, & Artal, 2004; Schwarz et al., 2014; Zheleznyak, Sabesan, Oh, MacRae, & Yoon, 2013). In fact, the use of AO visual simulators has allowed exploring different combinations of high order aberrations (HOAs) to expand DoF (i.e. primary and secondary spherical aberration (Yi et al., 2011) or astigmatism and coma (de Gracia et al., 2010). From these studies, it is concluded that not only the specific design, but also the native aberrations of the subjects and adaptation to them play a role in the multifocal performance with those lenses.

Multizonal refractive designs, in which certain pupillary regions are devoted for far and others for near, are also common. Multizonal lenses come most frequently in concentric areas, that typically alternate near and far zones (Sen, Sariikkola, Uusitalo, & Laatikainen, 2004). There is at least a refractive bifocal design with an asymmetric distribution of near and far, the Lentis Mplus (Oculentis, Germany), where the design approximates to a 2 segment bifocal with the rear surface add (+3.00 D) occupying almost half the lens (a sector enclosing an angle of ~ 160 deg) (Charman, 2014; Munoz, Albarran-Diego, Javaloy, Sakla, & Cervino, 2012; Plaza-Puche et al., 2015). The optimal pupillary distribution for far and near, and the extent to what a particular design interacts with the aberration pattern of the eye has been little addressed. However, previous studies have shown that a given optical design does not produce the same optical through-focus energy distributions in all eyes (Martin & Roorda, 2003). Among other parameters in bifocal lenses, the amount of near add largely determines visual quality both in terms of visual acuity (de Gracia, Dorronsoro, & Marcos, 2013) and perceived image quality (Radhakrishnan, Dorronsoro, Sawides, & Marcos, 2014). Besides, neural adaptation to simultaneous vision image has also been shown to shift perceived visual quality (Radhakrishnan et al., 2014).

Multifocal corrections (both intraocular and contact lenses) increase depth of focus at the expense of decreasing optical quality at all distances. While some studies have measured through-focus retinal image quality, generally using double-pass imaging techniques (Artal, Marcos, Navarro, Miranda, & Ferro, 1995; Kawamorita & Uozato, 2005; Navarro, Ferro, Artal, & Miranda, 1993) or visual quality (Gupta, Naroo, & Wolffsohn, 2009; Maxwell, Lane, & Zhou, 2009; Schmidinger et al., 2006; Woods, Woods, & Fonn, 2015), these are generally restricted to patients implanted or fitted with commercial lenses, and therefore limited to specific conditions. Most of the systematic evaluations of many of the available lenses are limited to optical computer simulations and on bench experiments, therefore lacking from the optical and the neural complexity of a patient (Martin & Roorda, 2003).

Computer simulations allow a first approximation to the understanding of the optical performance of multifocal lens designs. In a

recent study from our group, we computationally studied the through focus optical performance in diffraction-limited eyes with multi-zonal phase patterns, with 2–50 zones of varying power (maximum addition of +3 D) distributed either angularly or radially (de Gracia, Dorronsoro, & Marcos, 2013). Only some of these patterns roughly represent designs commercially available to date. Multifocality was evaluated in terms of two metrics, which considered the volume under the Visual Strehl through-focus curves in a certain dioptric range and the dioptric range for which through-focus Strehl exceeded a certain threshold. The study revealed clear differences in the predicted multifocality across lens designs, with 3- and 4-zone angular designs outperforming radial designs, or designs with more zones. Interestingly, the 50-zone radial designed provided almost identical performance to a spherical aberration pattern in the Visual Strehl (VS) through-focus curves, with lower VS values (by a factor of around 3) than most multizonal configurations of fewer zones. In a recent study, Legras et al. showed that subjects visually scored computer-generated images simulating the effect of multifocal segmented patterns with 2–20 zones, and found that through-focus perceived quality varied significantly across subjects (Legras & Rio, 2015). While in this study the subjective response of the subject was considered, the interaction between the subject's own aberrations and the multifocal profile did not occur as it would with a real correction.

Visual simulators allow testing experimentally different corrections, producing a real projection of the multifocal design in the pupil plane, and therefore a realistic interaction of the phase profile and eye's aberrations. In previous studies we evaluated experimentally visual perception with 14 different bifocal zonal corrections, using a custom-developed simultaneous vision simulator provided with a transmission Spatial Light Modulator (de Gracia, Dorronsoro, Sanchez-Gonzalez, Sawides, & Marcos, 2013; Dorronsoro, Radhakrishnan, de Gracia, Sawides, & Marcos, 2016; Dorronsoro et al., 2014; Radhakrishnan et al., 2014). All corrections had a 50% far–50% near energy balance and +3 D near add, with different angular and radial distributions. Subjects showed significant perceptual preferences across patterns. The same 2-zone angularly segmented pattern in different orientations produced significant differences in perception in the same subject, suggesting an influence of the interactions of the eye's aberration pattern and the multifocal pattern design.

AO simulators provide therefore the possibility of testing the influence of the eye's HOAs on the performance of multifocal corrections. To test visual performance with different multizone segmented patterns, we specifically developed a two-active-element Adaptive Optics system, provided with a deformable mirror that could compensate for the eye's aberrations, and a phase Spatial Light Modulators, which simulated multifocal (2, 3 and 4 zone) angular and zonal segmented phase designs. This study will help gain a better understanding of optical and visual interactions in multifocal simultaneous vision corrections, and whether these are driven by optical and neural effects, which is critical to improve intraocular lens design and select the optimal design for a patient.

2. Materials & methods

Visual quality with six phase designs (radial and angular segments) was evaluated optically and psychophysically, by means of simulations of Visual Strehl-based-metrics and measurements of the relative perceived visual quality, respectively.

2.1. Subjects

Six young subjects (ages ranging from 22 to 31 years, mean 29 ± 3.5 years) participated in the study. Spherical errors were

below ± 0.50 D (mean 0.10 ± 0.22 D), and astigmatism was ≤ -0.5 D in all cases. All experiments were conducted with cycloplegic eyes and paralyzed accommodation (by instillation of Tropicamide 1%, 2 drops 30 min prior to the beginning of the study, and 1 drop every 1 h).

All participants were acquainted with the nature and possible consequences of the study and provided written informed consent. All protocols met the tenets of the Declaration of Helsinki and had been previously approved by the Spanish National Research Council (CSIC) Ethical Committee.

2.2. Polychromatic Adaptive Optics setup

Perceived visual quality measurements were conducted in a custom-developed Adaptive Optics (AO) system at the Visual Optics and Biophotonics Lab (Institute of Optics, Spanish National Research Council), described partially in previous publications (Vinas, Dorransoro, Cortes, Pascual, & Marcos, 2015; Vinas, Dorransoro, Garzon, Poyales, & Marcos, 2015). The system allows measurement (Hartman-Shack aberrometry) and correction (with a deformable mirror) of HOAs, as well as simulation of segmented refractive multifocal patterns (with a Spatial Light Modulator), while performing psychophysical experiments.

The current configuration of the system (shown in a schematic diagram in Fig. 1) is formed by 6 different channels: the illumination Channel (I-Channel), with light coming from the supercontinuum laser source (SCLS) (red line); the AO-Channel (AO-Channel), whose main components are the Hartmann-Shack wavefront sensor and the deformable mirror (green line); the SLM-Channel

(SLM-Channel), which incorporates the Spatial Light Modulator (SLM) to the system (yellow line); the retinal imaging Channel (RI-Channel) (pink line); the pupil monitoring Channel (PM-Channel) (purple line); and the psychophysical Channel (PSY-Channel) (blue line). The system is mounted on an optical bench, whose physical dimensions are $900 \times 1800 \times 58$ mm.

The main components of the system are: (1) a Hartmann-Shack wavefront sensor (microlens array 40×32 , 3.6 mm effective diameter, centered at 1062 nm; HASO 32 OEM, Imagine Eyes, France), which measures the ocular aberrations (AO-Channel); (2) an electromagnetic deformable mirror (52 actuators, 15-mm effective diameter, 50- μ m stroke; MIRA0, Imagine Eyes, France), which corrects aberrations (AO-Channel); (3) a reflective LCOS (phase-only) Spatial Light Modulator (SLM; VIS; Resolution: 1920×1080 ; Pixel pitch: 8.0 μ m; Holoeye Photonics AG, Germany), which generates the multizone segmented phase designs (SLM-Channel); the deformable mirror, the wavefront sensor and the SLM are conjugated to the pupil by different relays of lenses. Magnification from the pupil is $2\times$ to the deformable mirror, $1\times$ to the SLM and $0.5\times$ to the wavefront sensor; (4) to display visual stimuli in the psychophysical channel a Digital Micro-Mirror Device (DMD), DLP[®] Discovery[™] 4100 0.7 XGA, Texas Instruments (USA), located in a retinal plane, monochromatically illuminated with light coming from the beam path through a holographic diffuser (HD) placed in the beam path breaks the coherence of the laser providing a uniform illumination of the stimulus, and subtending 1.62 degrees on the retina (PSY-Channel). The luminance of the stimulus was 20–25 cd/m^2 in the spectral range used for psychophysical testing (450–700 nm), therefore in the photopic region at all wavelengths;

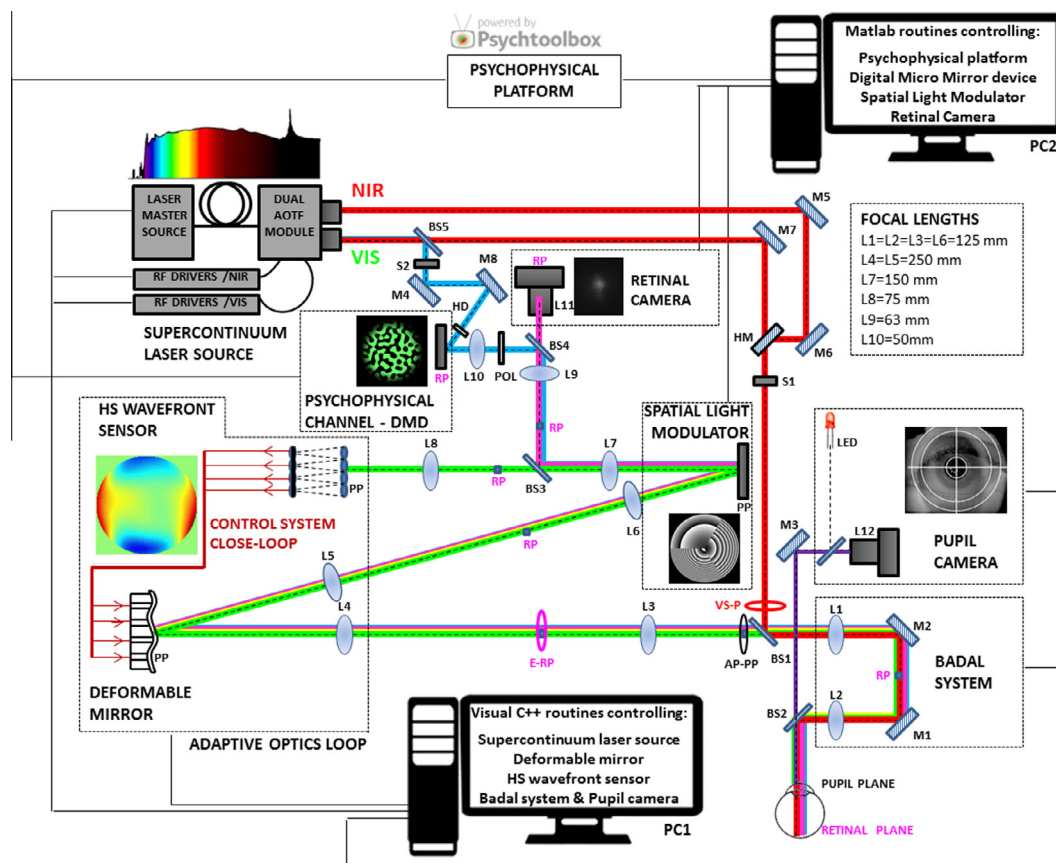


Fig. 1. Custom-made polychromatic adaptive-optics setup. Schematic diagram of the ViOBio Lab AO II system with the different channels in its final configuration (May, 2015): the illumination Channel (I-Channel, red line), the AO-Channel (green line); the SLM-Channel (yellow line); the retinal imaging Channel (RI-Channel, pink line); the pupil monitoring Channel (PM-Channel, purple line), and the psychophysical Channel (PSY-Channel, blue line). NIR: near infrared light; VIS: visible light; RP: retinal plane; PP: pupil plane; BS: beam splitter; S: shutter; L: lens; M: mirror; HM: hot mirror; POL: polarizer; E-RP: retinal pinhole; AP-PP: artificial pupil; VS-P: variable size pupil.

(5) A CCD camera (Retiga 1300, CCD Digital Camera, 12-bit, Monochrome, $6.7 \times 6.7 \mu\text{m}$ pixel size, 1024×1280 pixels; QImaging, Canada) provided with a collimating lens (L9, 63-mm focal length) and a camera lens (L11, 135-mm focal length) in the double-pass retinal imaging channel (RI-Channel). This channel captures retinal images, and it is not in use in the current experiment; (6) a Badal system which corrects for defocus in AO-, SLM- and PSY-Channels; and (7) a pupil monitoring channel (PM-Channel), which consists of a camera (DCC1545M, High Resolution USB2.0 CMOS Camera, Thorlabs GmbH, Germany) conjugated to the eye's pupil by means of an objective lens with 105-mm focal length (L12). Two automated shutters allow simultaneous illumination of the eye (S1) and the stimulus (S2).

All optoelectronic elements of the system (SCLS main source, Badal system, retinal image camera, pupil camera, Hartmann-Shack wavefront sensor, deformable mirror and Spatial Light Modulator) are automatically controlled and synchronized using custom-built software programmed in Visual C++ and C# (Microsoft). A dual acousto-optic modulator system, controlled with the software provided by the manufacturer, allowed automatic selection of the measurement wavelength. The custom-developed routines use the manufacturer's Software Development Kit for Hartmann-Shack centroiding detection and wave aberration polynomial fitting. Wave aberrations were fit by the 7th order Zernike polynomials and OSA convention was used for its ordering and normalization (Thibos, Applegate, Schwiegerling, & Webb, 2002).

Subjects are stabilized using a dental impression and are aligned to the system (using an x-y-z stage moving a bite bar) with the line of sight as a reference while the natural pupil is viewed on the monitor. To ensure proper pupil diameter during the measurements, a 6-mm artificial pupil was placed in a conjugate pupil plane.

2.3. Segmented multiple zone multifocal phase patterns

A total of six different refractive multizone segmented phase designs consisting of 2–4 segmented zones of progressive power (0 to +3.0 D, in equal discrete steps) were evaluated experimentally. Three patterns were angularly segmented and three patterns were radially segmented. Defocus (in a Zernike expansion) varied sequentially and linearly across zones between 0 and $-3.89 \mu\text{m}$ in a 6 mm pupil, equivalent to a dioptric power change from +0 D for far distance correction to +3.0 D for near (i.e., near addition). The angular lenses feature, N = 2, 3 and 4 zones of varying power across equi-sized sectors. The radial lenses again feature N = 2, 3 and 4 zones of varying power, where the zones are equal area concentric regions. The area of each zone was constant in all cases. Fig. 2 illustrates the designs (left) and corresponding phase patterns (right) tested in this study. Different colors represent different distributions of the far (green), near (red) and intermediate zones (orange). Grey scale images correspond to those used addressed in the SLM to represent the corresponding the phase patterns. Far (F) and Near (N) correspond in all designs to 0.0 D and +3.0 D respectively. For 3-zones designs (both radial and angular), Intermediate (I) corresponds to +1.5 D, while for 4-zones designs the 2 Intermediate zones correspond to +1.0D and +2.0 D respectively.

2.4. Perceived visual quality

A psychophysical experiment was designed to test the impact of the 6 different multizone segmented phase designs on vision, in patients with and without their natural aberrations. The aberrations were measured and manipulated, phase maps and the multifocal corrections generated, using a custom AO system.

2.4.1. Phase pattern generation

Matlab routines were used to numerically simulate the multizone segmented phase designs used experimentally, which were later programmed in a reflective LCoS (phase-only) Spatial Light Modulator. Each phase design is defined by the wavefront in each zone and a set of complementary masks (radial or angular, 2, 3 and 4 zones) that equals to 1 in the corresponding zone and 0 elsewhere (de Gracia, Dorronsoro, & Marcos, 2013). To replicate more realistic manufacturing conditions, a transition zone was incorporated to smooth the phase change between the different 3- and 4-angular segments (5 degrees). A wrapping process (Abdul-Rahman et al., 2007; Voelz, 2011) was applied to the phase patterns to achieve a maximum phase difference of 2π defined by the calibration of the SLM. The generated pattern was a grey-scale image, where each level of grey corresponds to a certain phase difference between 0 and 2π (Fig. 2). Images were generated for a 6-mm pupil at the pupil plane where the SLM is placed.

Calibration of the SLM was performed following the procedures indicated by the manufacturer for a wavelength of 555 nm. Cross-calibrations were performed between the different active-devices of the system (SLM, Deformable mirror and Badal system): different amounts of defocus were generated with the SLM and measured with the HS wavefront sensor, while the deformable mirror was set as to produce a flat wavefront and an artificial eye was placed in the pupil plane of the system. From the slopes of the calibration curve, a correction factor was calculated to modify the generated phase maps to obtain proper values of defocus measured with the HS wavefront sensor. For 555 nm the obtained correction factor was 1.338 ($R^2 = 0.99863$, slope of the calibration curve = 0.662).

2.4.2. Measurement protocol and psychophysical paradigm

Measurements were performed monocularly, without spectacle correction, in a darkened room. Spherical correction was subjectively set by the subject using a Badal optometer, while astigmatism and HOAs were measured and corrected with the deformable mirror in a closed loop Adaptive Optics operation. The state of the mirror that achieved HOAs correction was saved and applied during the measurements. Psychophysical measurements were performed at far, intermediate and near distances simulated with the Badal system (0 D, +1.5 D and +3.0 D from best distance spherical correction respectively), in the presence of natural aberrations and after AO-correction. Before the measurement, subjects were instructed on the nature of the experiment and performed some trial runs. A full measurement session lasted about 4 h.

Subject viewed the psychophysical stimulus generated by the Digital Micro-Mirror Device, illuminated monochromatically at 555 nm, through the psychophysical channel of the AO system (Fig. 1). The stimulus contained a binary noise pattern with sharp edges at random orientations, where the binary noise pattern was digitally produced from a uniform noise distribution spatially filtered with an annular filter in the frequency domain (inner radius: 3 cycles/deg; outer radius: 6 cycles/deg), that was later transformed to a binary image and smoothed by means of a Gaussian function (Chen, Singer, Guirao, Porter, & Williams, 2005). A new stimulus was generated on each trial with a different noise pattern, so that edges at all orientations were presented over the course of the experiment (see Fig. 1, psychophysical channel).

The psychophysical paradigm consisted on a two alternative forced-choice procedure (2AFC) weighted response to images viewed through 2 different multifocal patterns, in a series of 210 pairs of patterns, which is the number of permutation for all possible combination of pairs of the 6 designs (including the comparison of each pattern with itself) times 10 repetitions, at each distance. Patterns and viewing distances were randomly

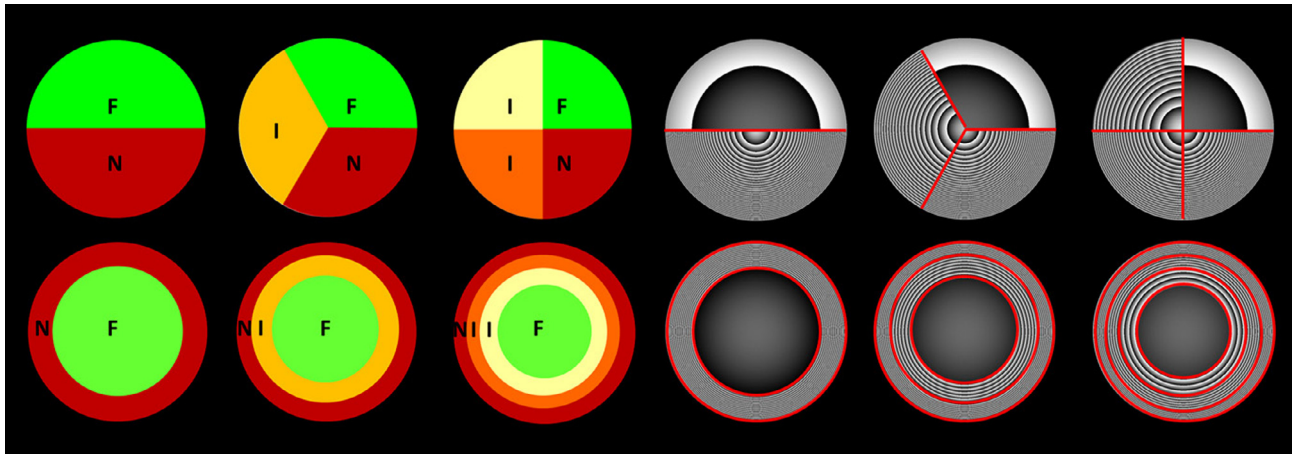


Fig. 2. Multizone angular and radial segmented phase designs evaluated in the study: 2, 3 and 4 zones angular (upper row) and radial (lower row) segmented designs. Left Panel; distribution of zones for Far (F, green, 0 D), Intermediate (I, yellow +1.0 D, dark orange +2.0 D D), and Near (N, red, +3.0 D) vision in the six multifocal designs (for 3-zones segmented designs I, light orange, stands for +1.5 D). Right Panel: multizone segmented phase maps as addressed in the SLM, for the six multifocal designs. For illustration, separation between zones has been highlighted.

selected. The subject viewed the stimuli and judged whether the first or second had better quality, and provided a ranked response according to the certainty of the judgment. Positively judged patterns received a score of +10, +5 and +1, and negatively judged patterns received a rank of –10, –5 and –1. The relative perceived visual quality of a given pattern is the sum of all responses to this pattern weighted by the corresponding scores. This procedure was done for each pattern, condition (natural and AO-corrected aberrations) and distance.

2.5. Optical quality

Fourier Optics was used to compute the through-focus optical quality for the different 6-zone angular and radial segmented phase designs. Natural aberrations of the 6 subjects measured with the AO system were incorporated to the optical simulations, as well as the residual aberrations after AO-correction, to study their impact on the optical performance.

2.5.1. Optical quality metrics

The Visual Strehl (VS) was used as an optical quality metric, estimated as the volume between the Modulation Transfer Function (MTF) of the system, and a general neural transfer function (Iskander, 2006; Marsack, Thibos, & Applegate, 2004). The MTF was estimated from the wave aberration and pupil function using Fourier Optics. Through-focus VS curves were calculated for all tested eyes and conditions (different multizone angular and radial segmented phase designs, with natural and AO-corrected aberrations). The following parameters were computed from the through-focus VS curves: (1) Area under VS curves in a 6.0 D dioptric range; (2) Dioptric range above a certain threshold (0.06); (3) VS at far, intermediate and near distance (0 D, 1.5 D and 3.0 D, respectively).

The response of an “ideal observer” purely responding on optical grounds to the same psychophysical test performed on subjects was calculated in all eyes, conditions and distances, from random comparisons of pattern pairs. A given pattern was deemed to produce better optical quality with weighting factors of ± 10 , ± 5 and ± 1 , if VS was 80%, 50% or 25% higher, respectively, than the corresponding pattern. A score for each pattern was calculated from the sum of the weighted responses, from a total of 210 comparisons. This estimation was similar to that obtained in patients from the corresponding psychophysical paradigm (see Section 2.4.2).

2.6. Data analysis

To test differences across multifocal designs, a multifocal benefit metric weighting the contribution of the different tested distances was built from the relative optical (ideal observer) and perceived visual quality results. The metric assigned a 60% weight to far distance data, 15% to intermediate distance and 25% to near distance.

Pattern preference results obtained with both methods, optical simulations and experimental measurements, at the different conditions (3 different distances, natural aberrations and AO correction) were organized in a ranking from 1 to 6, from the least preferred to the most preferred pattern, to allow comparison between both quality metrics.

3. Results

3.1. Wave aberration measurement and correction

Wave aberration maps for astigmatism and HOA and their corresponding RMS for all 6 subjects measured at 827 nm for a 6-mm pupil, for astigmatism and HOAs (purple), for astigmatism (yellow), for coma (pink) and residual aberrations after AO-correction (green) are shown in Fig. 3. Residual RMS upon AO-correction was lower than $0.05 \mu\text{m}$.

3.2. Perceived visual quality

The results of the perceptual responses of the 6 subjects participating in the study are summarized in Fig. 4. Perceived visual quality in the presence of natural aberrations (upper row) and after AO-correction of aberrations (lower row) for far (green bars), intermediate (red bars) and near (blue bars) vision. In 78.93% of the psychophysical pattern evaluations, a positive or negative statistically significant preference was found ($p < 0.05$; not compatible with chance), in pair comparisons with other patterns. In Fig. 4 empty bars stand for non-statistically significant results.

Fig. 5 shows the average (across 6 eyes) perceived visual quality obtained from pair comparisons in the corresponding psychophysical experiment, in the presence of natural aberrations (dashed bars) and after AO-correction (solid bars) for far (green bars), intermediate (red bars) and near (blue bars) vision. For far vision, 2-segmented designs (angular and radial) provided the better

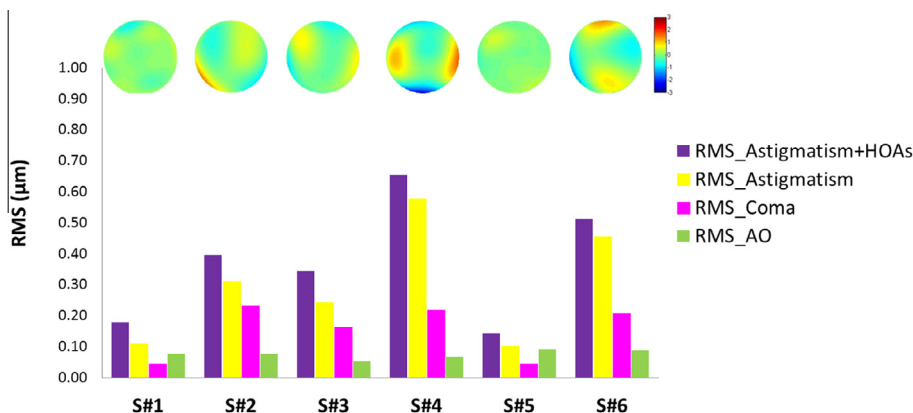


Fig. 3. Subject's wave aberration maps for HOAs (top) and Root Mean Square (RMS) for astigmatism and HOAs (purple), for astigmatism (yellow), for coma (pink) and residual aberrations after AO-correction (green). Data are for 6-mm pupil size.

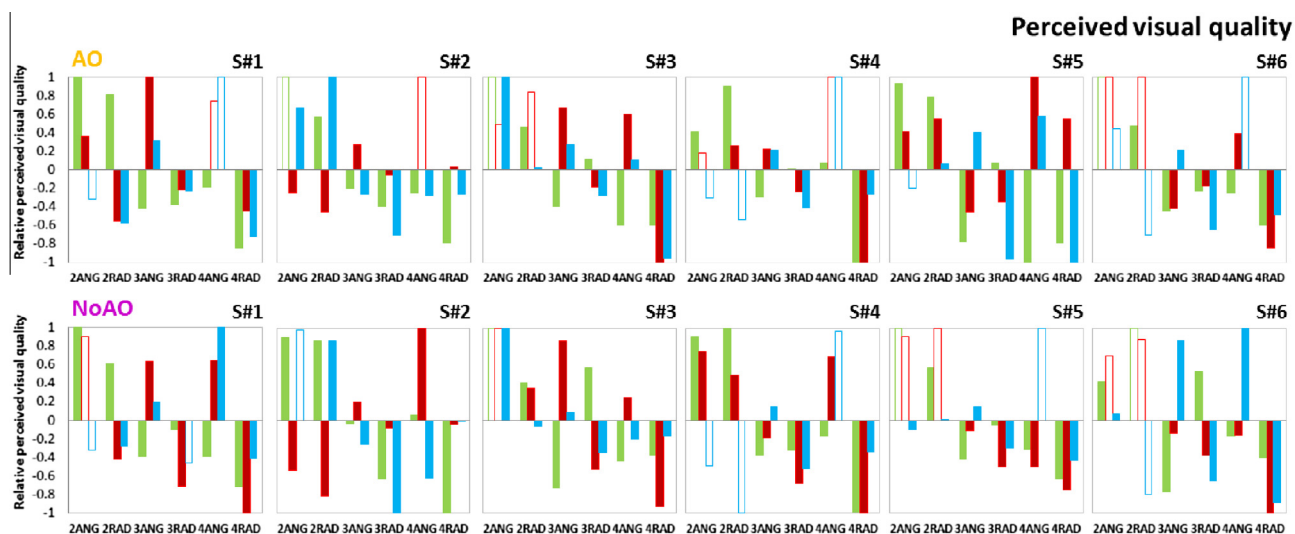


Fig. 4. Perceptual responses with each multifocal pattern from 6 subjects for far (green bars), intermediate (red bars) and near (blue bars) distance after AO-correction of natural aberrations (upper row) and in the presence of natural aberrations (lower row). Empty bars stands for non-significant values.

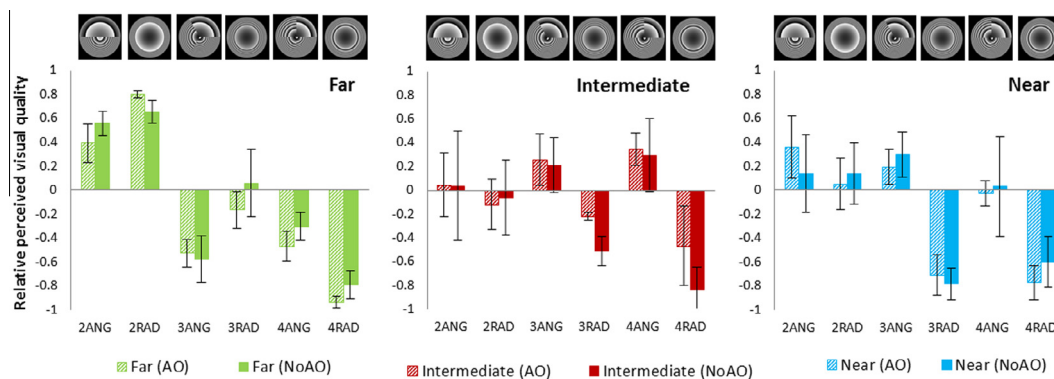


Fig. 5. Average relative perceived visual quality across 6 subjects with each multifocal pattern for far (green bars), intermediate (red bars) and near (blue bars) distance after AO-correction (dashed bars) and in the presence of natural aberrations (solid bars). Error bars stand for standard deviation across subjects. (For interpretation of the references to color in this figure legend, the reader is referred to the web version of this article.)

performance (Far: 2RAD 0.56, 2ANG 0.65), while for intermediate vision 3- and 4-zone angular segmented designs were optimal (Intermediate: 4ANG 0.29, 3ANG 0.21). For near vision, 2- and 3-zone angular segmented designs are preferred over the others

(Near: 3ANG 0.30, 2ANG 0.14, 2RAD 0.14). AO-correction of natural aberrations appears to have a minor impact on these trends. The presence of natural aberrations slightly increased the inter-subject variability (Far: 0.15; Intermediate: 0.27; Near:

0.25) in comparison with results with AO-correction (Far: 0.10; Intermediate: 0.20; Near: 0.17). Intersubject variability is lower for far distance and higher for intermediate distance.

3.3. Optical quality

Optical quality with the 6 different multizone segmented designs was obtained from optical simulations from wave aberrations measurements. The optical quality was computed from the combination of the multifocal phase map and the subject's aberrations (natural or residual after AO-correction). Fig. 6 shows an example of the corresponding wave aberrations for the tested designs (2, 3 and 4 angular and radial) and MTF radial profiles, for natural aberrations (upper row) and residual aberrations after AO-correction (lower row) in subject S#4. The corresponding PSFs have been included in an inverted grayscale in the upper right corner in each panel.

Through-focus VS curves, were calculated for all tested eyes and conditions and the following parameters computed: (1) Area under VS curves in a 6.0 D dioptric range (-1 D to $+5$ D); (2) Dioptric range above a certain threshold (0.06); (3) VS at far, intermediate and near distance (0 D, 1.5 D and 3.0 D, respectively). A threshold to normalize the area under the VS curves for each subject was set at the minimum value at intermediate distance (1.5 D) for 2-segmented designs through-focus curves.

Fig. 7 shows the simulated through-focus Visual Strehl (VS) curves for all 6 multizone segmented designs, for a diffraction limited eye (A) and in the presence of natural aberrations (angular (B-D) and radial (E-G)). Each color represents a different subject. Through-focus curves differ across designs, even for similar number of zones and no aberrations (A). The presence of natural aberrations produces variations from the diffraction-limited condition, including minor shifts in the maximum VS values, shifts in the curve peaks and variations in the performance of the same design across subjects.

Fig. 8 shows analysis of two different multifocal metrics (similar to those presented by de Gracia et al., 2013) for the different patterns, in a diffraction limited eye (open symbols) and average across subjects in the two conditions under test: natural aberrations (pink symbols) and residual aberrations (yellow symbols). The dashed squares indicate virgin eye performance. Fig. 8 plots the area under the VS through-focus curve between -1 D and $+5$ D as a function of the depth of focus (DoF), defined as the dioptric range for which VS is above the 0.06 threshold (de Gracia,

Dorrnsoro, & Marcos, 2013). For these particular metrics a better multifocal response is represented by higher values on both axes. In both conditions, 3- and 4-zone angular segmented designs produce better multifocal response than the rest of the tested multifocal designs.

Fig. 9 shows the average (across 6 eyes) relative optical quality (ideal observer) calculated from pair comparisons of the corresponding VS data, for three distances (far, intermediate and near). Simulations were performed in three conditions (diffraction limited eye, empty bars; residual aberrations following AO correction; natural aberrations, filled bars). For far and near distance, 2-zones segmented designs (angular and radial) provided better performance (Far: 2RAD 0.6, 2ANG 0.19; Near: 2ANG 0.61, 2RAD 0.44), while for intermediate vision, 3- and 4-zones segmented designs provided better performance, with angular designs performing better than the corresponding radial designs (Intermediate: 3ANG 0.65, 4ANG 0.59, 3RAD 0.40). AO-correction of natural aberrations has a small impact on these trends. These results were obtained for 6-mm pupil diameters. Simulations for 4.5-mm pupil diameters show similar results.

3.4. Optical vs. perceived visual quality

For comparison between optical (ideal observer) and perceived visual quality, the 6 patterns were organized in a ranking from 1 to 6, from the least preferred to the most preferred pattern on average. The ranking was done using the results of the optical simulations for far distance and AO correction, where the most preferred was 2RAD followed by 3RAD, 2ANG, 4RAD, 4 ANG and 3ANG. Fig. 10 shows the results of these rankings for the 3 testing distances (far: green, intermediate: red and near: blue) from the optical quality "ideal observer" calculations (squares, dashed lines) and perceived visual quality metric (triangles, solid lines) after AO-correction (upper row) and in the presence of natural aberrations (lower row). In general there is a good agreement between both optical predictions (ideal observer) and the psychophysical response for all distances in the presence of natural aberrations (RMS Ranking difference: Far: 0.41; Intermediate: 0.68; Near: 0.54) and after AO-correction (RMS Ranking difference: Far: 0.41; Intermediate: 0.54; Near: 0.41).

Multifocal benefit metrics were obtained from the relative optical quality (ideal observer) results and the relative visual quality results weighting the contribution of the different tested distances (60% weight to far distance data, 15% to intermediate distance and

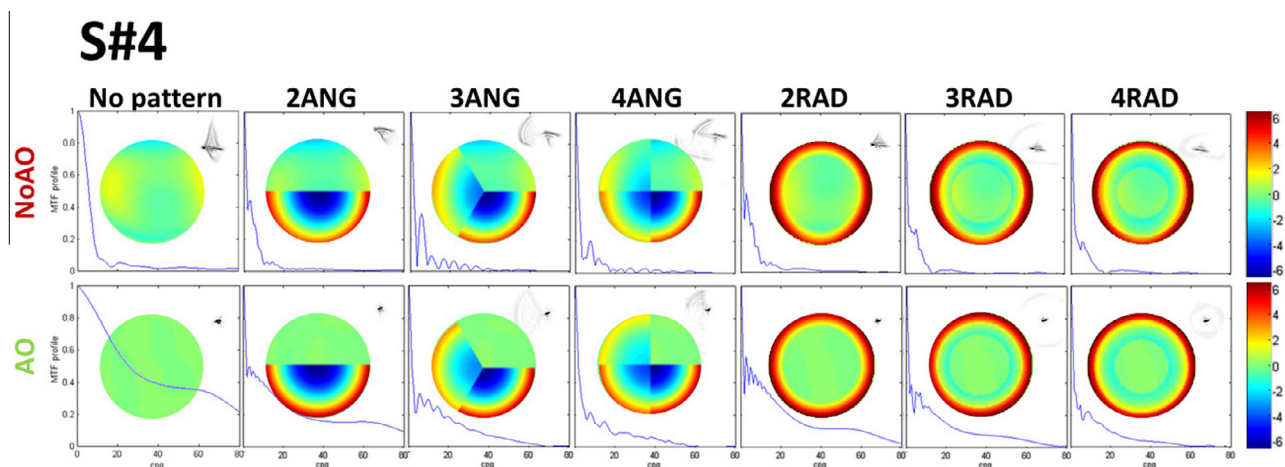


Fig. 6. Wave aberrations and corresponding MTF radial profiles and Point Spread Functions (PSFs) for the different conditions tested in the study, for 6-mm pupils. From left to right: no pattern (first column), 2, 3 and 4 segmented angular (left) and radial (right) segmented designs, for natural aberrations (upper row) and residual aberrations after AO-correction (lower row) in subject S#4 for far vision.

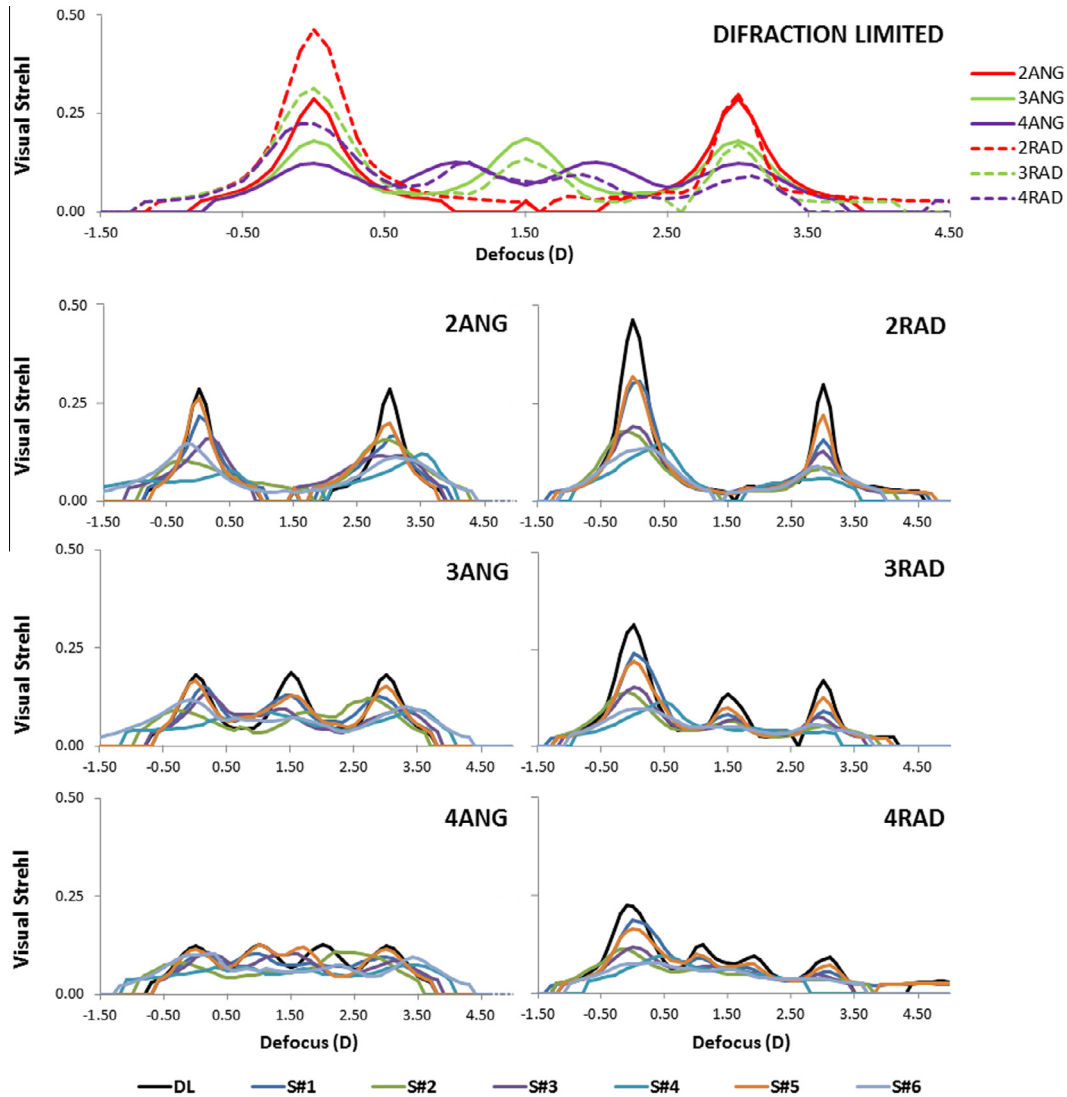


Fig. 7. Through-focus Visual Strehl curves for all 6 multizone segmented designs in a diffraction limited eye (upper panel), and angular and radial designs (lower panels) in the presence of natural aberrations, for 6-mm pupils.

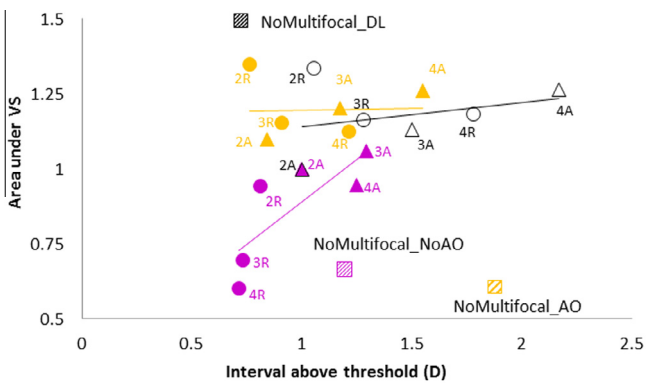


Fig. 8. Visual Strehl-based through-focus optical performance metrics for diffraction limited (black open symbols) and for the averaged data of the 6 subjects of the study. Pink symbols indicate data with natural aberrations and yellow symbols AO-corrected aberrations (Triangles stand for angular designs and circles for radial designs). The dashed squares stand for data without multifocal patterns (black diffraction-limited, pink natural aberrations, and yellow AO-corrected aberrations). The label besides each symbol represents the corresponding multifocal pattern. (For interpretation of the references to color in this figure legend, the reader is referred to the web version of this article.)

25% to near distance). Fig. 11 shows the multifocal benefit metric for all 6 subjects both from perceived visual quality (a and b) and optical quality (ideal observer) data (c and d) in the presence of natural aberrations (a and c) and after AO-correction (b and d). General trends are similar across subjects, with higher multifocal benefit obtained for 2-segmented designs, for both optical and perceived visual quality data.

Fig. 12 shows average results of the multifocal benefit metric obtained from the relative perceived quality results (dashed bars) and the optical quality (ideal observers) results (solid bars) in the presence of natural aberrations (right panel) and after AO-correction (left panel). General trends are similar with both metrics, although the optical predictions seem to overestimate the benefit of 3- and 4-zone designs, compared to the perceived quality.

4. Discussion

Multifocal optical corrections are becoming popular solutions for compensation of presbyopia, aiming at providing the patient with a range of focus for functional vision at near without compromising far vision (Cochener, Lafuma, Khoshnood,

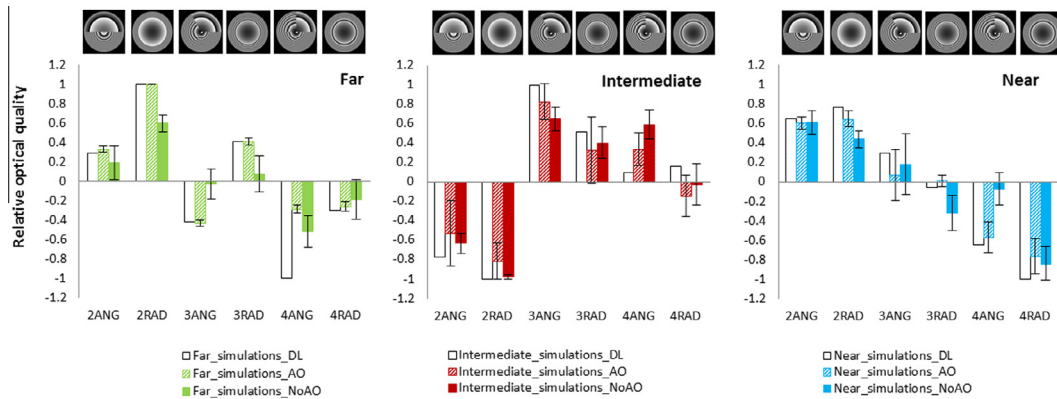


Fig. 9. Average responses across the 6 “Ideal observers” (i.e. purely based on the optical quality) with each multifocal pattern for far (green bars), intermediate (red bars) and near (blue bars) distance in the presence of natural aberrations (solid bars) and after AO-correction (dashed bars). Black empty bars are for diffraction-limited ideal observer for the 3 distances. Error bars stand for standard deviation across subjects. (For interpretation of the references to color in this figure legend, the reader is referred to the web version of this article.)

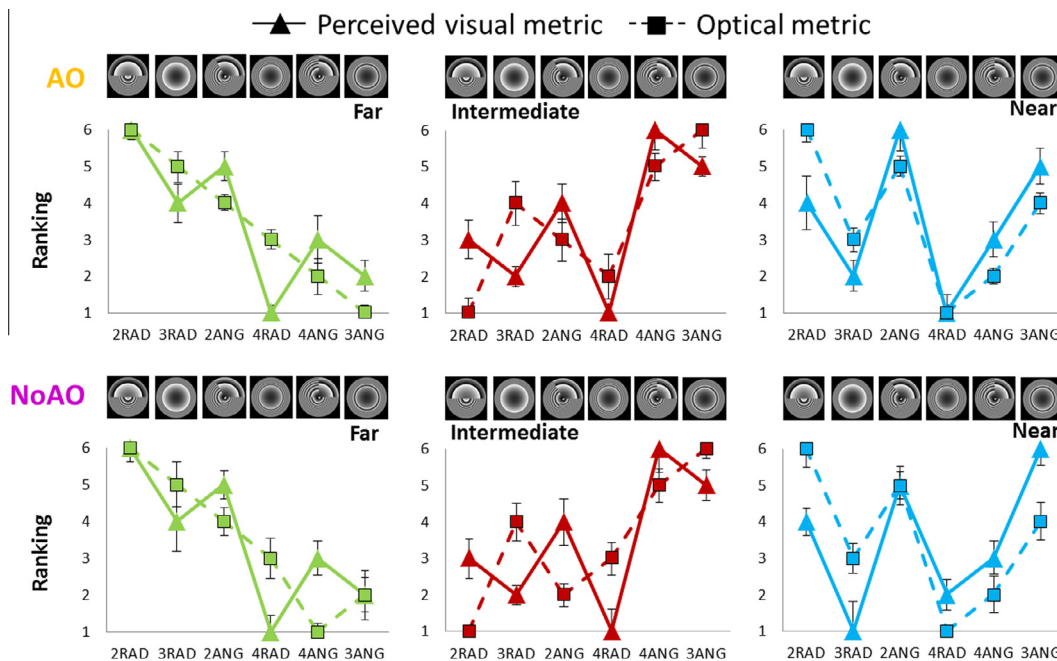


Fig. 10. Average rankings of multifocal patterns for the 3 testing distances (far: green, intermediate: red and near: blue) from optical predictions (ideal observer) (squares, dotted lines) and perceived visual quality (triangles, straight lines) after AO-correction (upper row and in the presence of natural aberrations (lower row). Error bars stand for standard deviation across subjects. (For interpretation of the references to color in this figure legend, the reader is referred to the web version of this article.)

Courouve, & Berdeaux, 2011; Kim, Zheleznyak, Macrae, Tchah, & Yoon, 2011; Lichtinger & Rootman, 2012). In the current study we have evaluated, optically (ideal observer) and psychophysically, the quality provided by six radial and angularly segmented multiple zone multifocal phase patterns. Optical quality was evaluated by means of Visual Strehl-based-metrics and relative visual quality was obtained by means of a psychophysical paradigm in which subject judged perceptually images viewed through 210 pairs of patterns. For that purpose we have developed a two-active-element AO system provided with a deformable mirror that could compensate for the eye’s aberrations, and a phase SLM, which simulated multifocal (2, 3 and 4 zone) angular and zonal patterns to allow a better understanding of optical and visual interactions in multifocal simultaneous vision corrections. In general, we found that 2-zone designs outperformed other designs in an overall multifocality metric (Figs. 11 and 12), matching the performance of a simulated ideal observer with purely optically-based responses.

On the other hand, 3–4 zone designs that include intermediate power show a preference for intermediate vision, favoring angular over radial patterns. These experiments suggest the utility of the adaptive-optics visual simulator to capture subtleties across different multifocal designs, and its potential for optimizing the multifocal correction selection.

A previous study from our laboratory (de Gracia, Dorronsoro, & Marcos, 2013) studied computationally the multifocal performance in diffraction-limited eyes with different multifocal designs using a combined metric that considered the volume under the Visual Strehl through-focus curves in a certain dioptric range and the dioptric range for which through-focus Strehl exceeded a certain threshold. The study revealed clear differences in the predicted multifocality across lens designs, with 3- and 4-zone angular designs outperforming radial designs, or designs with more zones. In the current study, we have found similar trends for those metrics in eyes with real aberrations (Fig. 8).

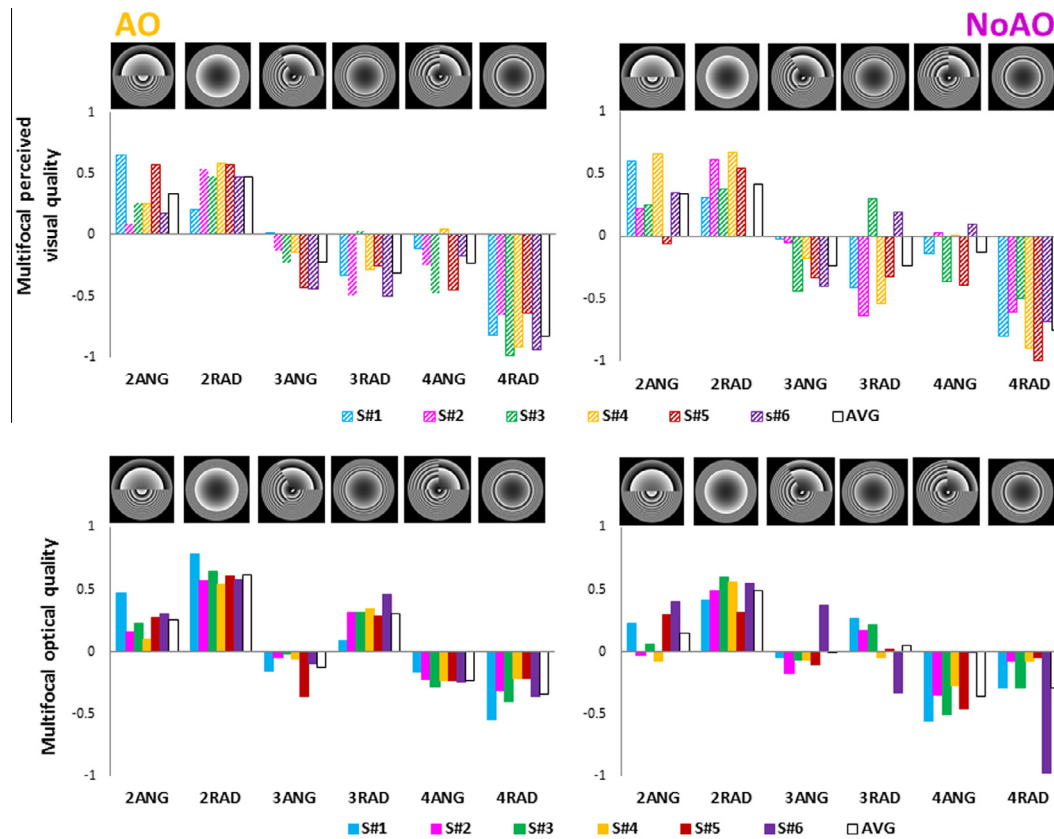


Fig. 11. Multifocal perceived visual quality (upper row) and multifocal optical quality (ideal observer) (lower row) in the presence of natural aberrations (left column) and after AO-correction (right column) for all 6 subjects participating in the experiment.

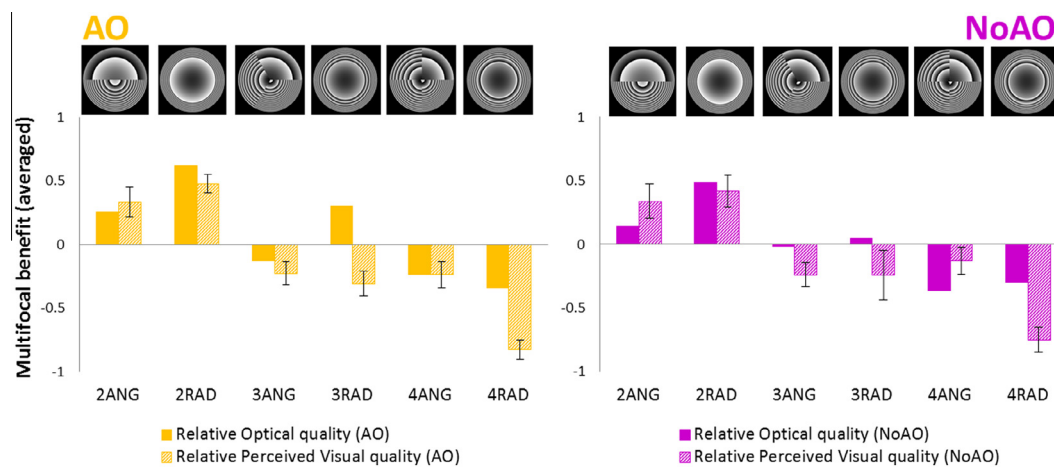


Fig. 12. Average multifocal benefit metric across 6 subjects with each multifocal pattern from optical predictions (ideal observer) (solid bars) and perceived visual quality (dashed bars) with AO-correction (right panel) and natural aberrations (left panel) for the 6 different multifocal patterns. Error bars represent standard deviations across subjects.

The pattern-comparison tests (both optical and psychophysical), showed that while 2-segmented designs (angular and radial) provided better performance for far and near vision, 3- and 4-zone angular designs performed better for intermediate vision (Fig. 9), and over-performed the same-zone radial designs. AO-correction of natural aberrations of the subjects modified the response for the different subjects but general trends remained. A comparison of these findings with the multifocality metrics based on the dioptric range above threshold and the area under

the VS curves indicate that these metrics favor designs with intermediate powers. With a multifocal benefit metric that integrated the relative perceived quality at near, intermediate and far distances, the optical simulations predicted very closely the visual response for most multifocal designs, for both AO-corrected and natural aberrations. The largest discrepancies between perceptually measured and optically predicted multifocal benefit occurred systematically for 3 and 4 radial designs. We can only speculate on the origin of this difference, which might be

associated to the Stiles–Crawford induced radial changes in pupillary efficiency, perhaps more relevant for increased number of zones.

Our results indicate that the design (angular or radial) of the multifocal solution has greater impact on vision than the presence/absence of natural aberrations of the subject, even when the natural aberrations are AO-corrected. However differences in perceived visual quality across subjects (Fig. 4) showed that the best optical design for each subject might be driven by his/her neural adaptation to his/her natural aberrations. AO-correction of natural aberrations slightly reduced the intersubject variability and had reduced impact on general trends, however they might have some implications and seem to play some role and should be considered when customizing a design for a particular subject.

Visual simulation with Adaptive Optics (de Gracia et al., 2010; Piers et al., 2004; Schwarz et al., 2014; Yi et al., 2011; Zheleznyak et al., 2013) allows identifying the optimal multifocal correction for a patient, the effects of interactions of the natural aberrations and a better understanding of the role played by aberrations in perceived visual quality across different multifocal patterns. The Adaptive Optics Visual Simulator developed in the current study allows evaluating vision with any multifocal solution, while controlling the natural aberrations of the subject to allow a better understanding of optical and visual interactions in multifocal simultaneous vision corrections, and to investigate whether these interactions are driven by optical or by neural effects, which is critical to improve intraocular lens design and to select the optimal design for a patient. However some concerns have been raised when simulating phase pattern designs by means of a phase-only reflective SLM to evaluate visual function with optical designs with abrupt phase changes. For that reason, further work is needed to evaluate visual function with simulated phase designs, with an SLM, and through the same designs manufactured on a physical phase plate.

Commercial relationships

None.

Acknowledgments

This research has been funded by the European Research Council under the European Union's Seventh Framework Program (FP/2007–2013)/ERC Grant Agreement [ERC-2011–AdC 294099]. This study was also supported by Spanish Government grants FIS2011–25637 & FIS2014–56643–R to SM and CSIC JAE-Pre programs & MICINN FPU Predoctoral Fellowship to MV.

References

- Abdul-Rahman, H. S., Gdeisat, M. A., Burton, D. R., Lalor, M. J., Lilley, F., & Moore, C. J. (2007). Fast and robust three-dimensional best path phase unwrapping algorithm. *Applied Optics*, 46(26), 6623–6635.
- Artal, P., Marcos, S., Navarro, R., Miranda, I., & Ferro, M. (1995). Through focus image quality of eyes implanted with monofocal and multifocal intraocular lenses. *Optical Engineering*, 34(3), 772–779.
- Charman, W. N. (2014). Developments in the correction of presbyopia II: Surgical approaches. *Ophthalmic and Physiological Optics*, 34(4), 397–426.
- Chen, L., Singer, B., Guirao, A., Porter, J., & Williams, D. R. (2005). Image metrics for predicting subjective image quality. *Optometry and Vision Science*, 82(5), 358–369.
- Cochener, B., Lafuma, A., Khoshnood, B., Courouve, L., & Berdeaux, G. (2011). Comparison of outcomes with multifocal intraocular lenses: A meta-analysis. *Clinical Ophthalmology*, 5, 45–56.
- Davison, J. A., & Simpson, M. J. (2006). History and development of the apodized diffractive intraocular lens. *Journal of Cataract and Refractive Surgery*, 32(5), 849–858.

- de Gracia, P., Dorronsoro, C., Gamba, E., Marin, G., Hernandez, M., & Marcos, S. (2010). Combining coma with astigmatism can improve retinal image over astigmatism alone. *Vision Research*, 50(19), 2008–2014.
- de Gracia, P., Dorronsoro, C., & Marcos, S. (2013a). Multiple zone multifocal phase designs. *Optics Letters*, 38(18), 3526–3529.
- de Gracia, P., Dorronsoro, C., Sanchez-Gonzalez, A., Sawides, L., & Marcos, S. (2013b). Experimental simulation of simultaneous vision. *Investigative Ophthalmology & Visual Science*, 54(1), 415–422.
- Dorronsoro, C., Gonzalez-Anera, R., Gonzalez, M.J., Llorente, L., & Marcos, S. (2004). Development of an experimental model on artificial corneas for the study of adaptation and optical quality of contact lenses. In *2nd European optical society topical meeting on physiological optics* (Granada, Spain).
- Dorronsoro, C., Radhakrishnan, A., de Gracia, P., Sawides, L., & Marcos, S. (2016). Perceived image quality with different experimentally simulated segmented bifocal corrections. Submitted.
- Dorronsoro, C., Radhakrishnan, A., de Gracia, P., Sawides, L., Alonso-Sanz, J. R., Cortés, D., & Marcos, S. (2014). Visual testing of segmented bifocal corrections with a compact simultaneous vision simulator. *Investigative Ophthalmology & Visual Science*, 55(13), 781–781.
- Fernandez, D., Barbero, S., Dorronsoro, C., & Marcos, S. (2013). Multifocal intraocular lens providing optimized through-focus performance. *Optics Letters*, 38(24), 5303–5306.
- Gatinel, D., Pagnouille, C., Houbrechts, Y., & Gobin, L. (2011). Design and qualification of a diffractive trifocal optical profile for intraocular lenses. *Journal of Cataract and Refractive Surgery*, 37(11), 2060–2067.
- Glasser, A., & Campbell, M. C. (1998). Presbyopia and the optical changes in the human crystalline lens with age. *Vision Research*, 38(2), 209–229.
- Gupta, N., Naroo, S. A., & Wolffsohn, J. S. (2009). Visual comparison of multifocal contact lens to monovision. *Optometry and Vision Science*, 86(2), E98–E105.
- Iskander, D. R. (2006). Computational aspects of the visual Strehl ratio. *Optometry and Vision Science*, 83(1), 57–59.
- Kawamori, T., & Uozato, H. (2005). Modulation transfer function and pupil size in multifocal and monofocal intraocular lenses in vitro. *Journal of Cataract and Refractive Surgery*, 31(12), 2379–2385.
- Kim, M. J., Zheleznyak, L., Macrae, S., Tchah, H., & Yoon, G. (2011). Objective evaluation of through-focus optical performance of presbyopia-correcting intraocular lenses using an optical bench system. *Journal of Cataract and Refractive Surgery*, 37(7), 1305–1312.
- Legras, R., & Rio, D. (2015). Effect of number of zones on subjective vision in concentric bifocal optics. *Optometry and Vision Science*, 92(11), 1056–1062.
- Lichtinger, A., & Rootman, D. S. (2012). Intraocular lenses for presbyopia correction: Past, present, and future. *Current Opinion in Ophthalmology*, 23(1), 40–46.
- Marsack, J. D., Thibos, L. N., & Applegate, R. A. (2004). Metrics of optical quality derived from wave aberrations predict visual performance. *Journal of Vision*, 4(4), 322–328.
- Martin, J. A., & Roorda, A. (2003). Predicting and assessing visual performance with multizone bifocal contact lenses. *Optometry and Vision Science*, 80(12), 812–819.
- Maxwell, W. A., Lane, S. S., & Zhou, F. (2009). Performance of presbyopia-correcting intraocular lenses in distance optical bench tests. *Journal of Cataract and Refractive Surgery*, 35(1), 166–171.
- Mojzis, P., Majerova, K., Hrcakova, L., & Pinero, D. P. (2015). Implantation of a diffractive trifocal intraocular lens: One-year follow-up. *Journal of Cataract and Refractive Surgery*, 41(8), 1623–1630.
- Munoz, G., Albarran-Diego, C., Javaloy, J., Sakla, H. F., & Cervino, A. (2012). Combining zonal refractive and diffractive aspheric multifocal intraocular lenses. *Journal of Refractive Surgery*, 28(3), 174–181.
- Navarro, R., Ferro, M., Artal, P., & Miranda, I. (1993). Modulation transfer functions of eyes implanted with intraocular lenses. *Applied Optics*, 32(31), 6359–6367.
- Piers, P. A., Fernandez, E. J., Manzanera, S., Norrby, S., & Artal, P. (2004). Adaptive optics simulation of intraocular lenses with modified spherical aberration. *Investigative Ophthalmology & Visual Science*, 45(12), 4601–4610.
- Plaza-Puche, A. B., Alio, J. L., MacRae, S., Zheleznyak, L., Sala, E., & Yoon, G. (2015). Correlating optical bench performance with clinical defocus curves in varifocal and trifocal intraocular lenses. *Journal of Refractive Surgery*, 31(5), 300–307.
- Radhakrishnan, A., Dorronsoro, C., Sawides, L., & Marcos, S. (2014). Short-term neural adaptation to simultaneous bifocal images. *PLoS ONE*, 9(3), e93089.
- Schmidinger, G., Geitzenauer, W., Hahsle, B., Klemen, U. M., Skorpik, C., & Pieh, S. (2006). Depth of focus in eyes with diffractive bifocal and refractive multifocal intraocular lenses. *Journal of Cataract and Refractive Surgery*, 32(10), 1650–1656.
- Schwarz, C., Canovas, C., Manzanera, S., Weeber, H., Prieto, P. M., Piers, P., & Artal, P. (2014). Binocular visual acuity for the correction of spherical aberration in polychromatic and monochromatic light. *Journal of Vision*, 14(2).
- Sen, H. N., Sariikkola, A. U., Uusitalo, R. J., & Laatikainen, L. (2004). Quality of vision after AMO Array multifocal intraocular lens implantation. *Journal of Cataract and Refractive Surgery*, 30(12), 2483–2493.
- Thibos, L. N., Applegate, R. A., Schwiegerling, J. T., & Webb, R. (2002). Standards for reporting the optical aberrations of eyes. *Journal of Refractive Surgery*, 18(5), S652–S660.
- Vinas, M., Dorronsoro, C., Cortes, D., Pascual, D., & Marcos, S. (2015a). Longitudinal chromatic aberration of the human eye in the visible and near infrared from wavefront sensing, double-pass and psychophysics. *Biomedical Optics Express*, 6(3), 948–962.
- Vinas, M., Dorronsoro, C., Garzon, N., Poyales, F., & Marcos, S. (2015b). In vivo subjective and objective longitudinal chromatic aberration after bilateral

- implantation of the same design of hydrophobic and hydrophilic intraocular lenses. *Journal of Cataract and Refractive Surgery*, 41(10), 2115–2124.
- Voelz, D.G. (2011). Computational Fourier optics: A MATLAB tutorial. SPIE.
- Woods, J., Woods, C., & Fonn, D. (2015). Visual performance of a multifocal contact lens versus monovision in established presbyopes. *Optometry and Vision Science*, 92(2), 175–182.
- Yi, F., Iskander, D. R., & Collins, M. (2011). Depth of focus and visual acuity with primary and secondary spherical aberration. *Vision Research*, 51(14), 1648–1658.
- Zheleznyak, L., Sabesan, R., Oh, J. S., MacRae, S., & Yoon, G. (2013). Modified monovision with spherical aberration to improve presbyopic through-focus visual performance. *Investigative Ophthalmology & Visual Science*, 54(5), 3157–3165.